



Observation of charmonium pairs produced exclusively in pp collisions

The LHCb collaboration[†]

Abstract

A search is performed for the central exclusive production of pairs of charmonia produced in proton-proton collisions. Using data corresponding to an integrated luminosity of 3 fb^{-1} collected at centre-of-mass energies of 7 and 8 TeV, $J/\psi J/\psi$ and $J/\psi \psi(2S)$ pairs are observed, which have been produced in the absence of any other activity inside the LHCb acceptance that is sensitive to charged particles in the pseudorapidity ranges $(-3.5, -1.5)$ and $(1.5, 5.0)$. Searches are also performed for pairs of P-wave charmonia and limits are set on their production. The cross-sections for these processes, where the dimeson system has a rapidity between 2.0 and 4.5, are measured to be

$$\begin{aligned}
 \sigma^{J/\psi J/\psi} &= 58 \pm 10(\text{stat}) \pm 6(\text{syst}) \text{ pb}, \\
 \sigma^{J/\psi \psi(2S)} &= 63_{-18}^{+27}(\text{stat}) \pm 10(\text{syst}) \text{ pb}, \\
 \sigma^{\psi(2S)\psi(2S)} &< 237 \text{ pb}, \\
 \sigma^{\chi_{c0}\chi_{c0}} &< 69 \text{ nb}, \\
 \sigma^{\chi_{c1}\chi_{c1}} &< 45 \text{ pb}, \\
 \sigma^{\chi_{c2}\chi_{c2}} &< 141 \text{ pb},
 \end{aligned}$$

where the upper limits are set at the 90% confidence level. The measured $J/\psi J/\psi$ and $J/\psi \psi(2S)$ cross-sections are consistent with theoretical expectations.

Submitted to Journal of Physics G

© CERN on behalf of the LHCb collaboration, license CC-BY-4.0.

[†]Authors are listed at the end of the paper.

1 Introduction

Central exclusive production (CEP), $pp \rightarrow pXp$, in which the protons remain intact and the system X is produced with a rapidity gap on either side, requires the exchange of colourless propagators, either photons or combinations of gluons that ensure a net neutral colour flow. CEP provides an attractive laboratory in which to study quantum chromodynamics (QCD) and the role of the pomeron, particularly when the mass of the central system is high enough to allow perturbative calculations [1]. Furthermore, it presents an opportunity to search for exotic states in a low-background experimental environment.

CEP has been studied at hadron colliders from the ISR to the Tevatron. At the LHC, measurements of exclusive single J/ψ photoproduction have been made by the LHCb [2] and ALICE [3] collaborations. The CEP of vector meson pairs has been measured in $\omega\omega$ [4] and $\phi\phi$ [5, 6] channels by the WA102 and WA76 collaborations. In this paper, CEP of S-wave, $J/\psi J/\psi$, $J/\psi\psi(2S)$, $\psi(2S)\psi(2S)$, and P-wave, $\chi_{c0}\chi_{c0}$, $\chi_{c1}\chi_{c1}$, $\chi_{c2}\chi_{c2}$, charmonium pairs are examined for the first time, using a data sample corresponding to an integrated luminosity of about 3 fb^{-1} , collected by the LHCb experiment.

Investigations of the cross-sections and invariant mass spectra of charmonium pairs are sensitive to the presence of additional particles in the decay chain such as glueballs or tetraquarks [7]. LHCb has measured the inclusive production of J/ψ pairs [8] in broad agreement with the QCD predictions, although the invariant mass distribution of the dimeson system is shifted to higher values in data. In the inclusive case, this shift could be an indication of double parton scattering (DPS) effects [9]. In CEP however, DPS through photoproduction is negligible due to the peripheral nature of the collision. Thus, a comparison of the mass spectra in inclusive and exclusive production gives further information for understanding J/ψ pair production.

The principal production mechanism for the CEP of two charmonia is through double pomeron exchange (DPE) as shown in the left diagram of Fig. 1, where one t-channel gluon participates in the hard interaction and the second (soft) gluon shields the colour

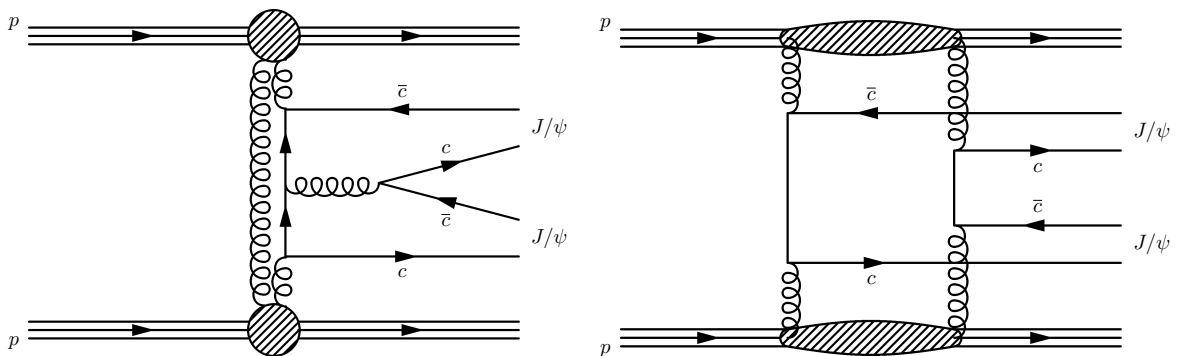


Figure 1: Representative Feynman diagrams for pairs of charmonia produced through double pomeron exchange. In the left, one t -channel gluon is much softer than the other while in the right, they are similar.

charge. Using the Durham model [10], this can be related to the $gg \rightarrow J/\psi J/\psi$ process calculated in Refs. [7, 11]. Another mechanism [12] that may lead to higher dimeson masses and an enhanced cross-section is shown in the right diagram of Fig. 1.

Several theory papers consider the production of pairs of charmonia by two-photon fusion [13–18], which is of importance in heavy-ion collisions and at high-energy e^+e^- colliders. However, in pp interactions DPE dominates. A recent work [12] gives predictions for the DPE production of light meson pairs, which are implemented in the SUPERCHIC generator [19]. The formalism can be extended to obtain predictions for charmonium pairs.

2 Detector and data samples

The LHCb detector [20] is a single-arm forward spectrometer covering the pseudorapidity range $2 < \eta < 5$ (forward region), primarily designed for the study of particles containing b or c quarks. The detector includes a high-precision tracking system consisting of a silicon-strip vertex detector (VELO) [21] surrounding the pp interaction region, a large-area silicon-strip detector located upstream of a dipole magnet with a bending power of about 4 Tm, and three stations of silicon-strip detectors and straw drift tubes [22] placed downstream of the magnet. The tracking system provides a measurement of momentum with a relative uncertainty that varies from 0.4% at low momentum to 0.6% at 100 GeV.¹ The minimum distance of a track to a primary vertex, the impact parameter, is measured with a resolution of $(15 + 29/p_T) \mu\text{m}$, where p_T is the component of momentum transverse to the beam, in GeV. In addition, the VELO has sensitivity to charged particles with momenta above ~ 100 MeV in the pseudorapidity range $-3.5 < \eta < -1.5$ (backward region), while extending the sensitivity of the forward region to $1.5 < \eta < 5$.

Different types of charged hadrons are distinguished using information from two ring-imaging Cherenkov detectors [23]. Photon, electron and hadron candidates are identified by a calorimeter system consisting of scintillating-pad (SPD) and pre-shower detectors, an electromagnetic calorimeter and a hadronic calorimeter. The SPD also provides a measure of the charged particle multiplicity in an event. Muons are identified by a system composed of alternating layers of iron and multiwire proportional chambers [24]. The trigger [25] consists of a hardware stage, based on information from the calorimeter and muon systems, followed by a software stage, which applies a full event reconstruction.

The data used in this analysis correspond to an integrated luminosity of $946 \pm 33 \text{ pb}^{-1}$ collected in 2011 at a centre-of-mass energy $\sqrt{s} = 7 \text{ TeV}$ and $1985 \pm 69 \text{ pb}^{-1}$ collected in 2012 at $\sqrt{s} = 8 \text{ TeV}$. The two datasets are combined because the overall yields are low and the cross-sections are expected to be similar at the two energies. The J/ψ and $\psi(2S)$ mesons are identified through their decays to two muons, while the χ_c mesons are searched for in the decay channels $\chi_c \rightarrow J/\psi \gamma$. The protons are only marginally deflected by the peripheral collision and remain undetected inside the beam pipe. Therefore, the signature for exclusive charmonium pairs is an event containing four muons, at most two photons, and no other activity. Beam-crossings with multiple proton interactions produce

¹Natural units are used throughout this paper.

additional activity; in the 2011 (2012) data-taking period the average number of visible interactions per bunch crossing was 1.4 (1.7). Requiring an exclusive signature restricts the analysis to beam crossings with a single pp interaction.

Simulated events are used primarily to determine the detector acceptance. No generator has implemented exclusive J/ψ pair production; therefore, the dimeson system is constructed with the mass and transverse momentum distribution observed in the data, and the rapidity distribution as predicted for DPE processes by the Durham model [10]. Systematic uncertainties associated with this procedure are discussed in Sec. 5. The dimeson system is forced to decay, ignoring spin and polarisation effects, using the PYTHIA generator [26] and passed through a GEANT4 [27] based detector simulation, the trigger emulation and the event reconstruction chain of the LHCb experiment.

3 Event selection and yields

The hardware trigger used in this analysis requires a single muon candidate with transverse momentum $p_T > 400$ MeV in coincidence with a low SPD multiplicity (< 10 hits). The software trigger used to select signal events requires two muons with $p_T > 400$ MeV.

The analysis is performed in the fiducial region where the dimeson system has a rapidity between 2.0 and 4.5. The selection of pairs of S-wave charmonia begins by requiring four reconstructed tracks that incorporate VELO information, for which the acceptance is about 30%. At least three tracks are required to be identified as muons. It is required that there are no photons reconstructed in the detector and no other tracks that have VELO information.

The invariant masses of oppositely charged muon candidates is shown in the left plot of Fig. 2. Accumulations of events are apparent around the J/ψ and $\psi(2S)$ masses.

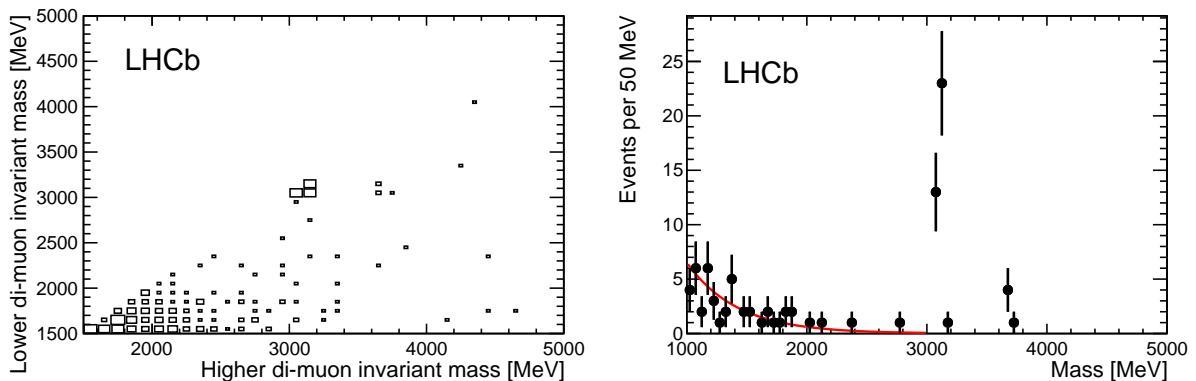


Figure 2: Left: Invariant masses of pairs of oppositely charged muons in events with exactly four tracks. Of the two possible ways of combining the muons per event, the one with the higher value for the lower-mass pair is plotted. Right: Invariant mass of the second pair of tracks where the first pair has a mass consistent with the J/ψ or $\psi(2S)$ meson. When both masses are consistent with a charmonium, only the candidate with the higher mass is displayed. The curve shows an exponential fit in the region below 2500 MeV.

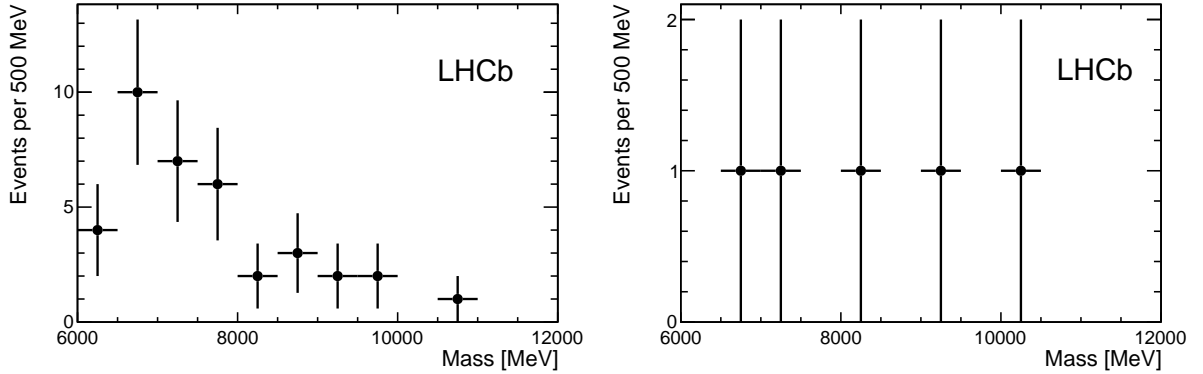


Figure 3: Invariant mass of the four-muon system in (left) $J/\psi J/\psi$ and (right) $J/\psi \psi(2S)$ events.

Requiring that one of the masses is within -200 MeV and $+65$ MeV of the known J/ψ or $\psi(2S)$ mass [28], the invariant mass of the other two tracks is shown in the right plot of Fig. 2. Clear signals are observed about the J/ψ and $\psi(2S)$ masses and candidates within -200 MeV and $+65$ MeV of their masses are selected. There are 37 $J/\psi J/\psi$ candidates, 5 $J/\psi \psi(2S)$ candidates, and no $\psi(2S)\psi(2S)$ candidates. Although it is not explicitly required in the selection, all candidates are consistent with originating from a single vertex. The invariant mass distributions of the four-muon system in $J/\psi J/\psi$ and $J/\psi \psi(2S)$ events are shown in Fig. 3. The shape of the $J/\psi J/\psi$ mass distribution is consistent with that observed in the inclusive analysis [8].

The events selected here are produced through a different production mechanism than those selected in the inclusive analysis of J/ψ pairs, as can be appreciated by examining the charged multiplicity distributions. The inclusive signal has an average multiplicity of 190 reconstructed tracks, with only 2 (0.2)% of events having multiplicities below 50 (20). In contrast, Fig. 4 shows the number of tracks, in triggered events with a low SPD multiplicity, for the selection of exclusive $J/\psi J/\psi$ events when the requirements on no additional activity

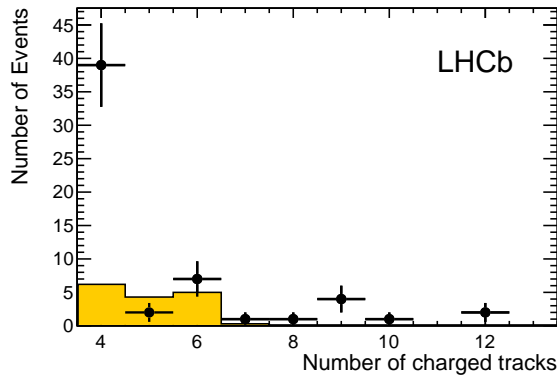


Figure 4: Number of tracks passing the $J/\psi J/\psi$ exclusive selection after having removed the requirement that there be no additional charged tracks or photons. The shaded histogram is the expected feed-down from exclusive $J/\psi \psi(2S)$ events.

(either extra tracks or photons) is removed. The peak at four tracks is noteworthy. A small peak of 7 events with six tracks is consistent with the expected number of exclusive $J/\psi\psi(2S)$ events, where $\psi(2S) \rightarrow J/\psi\pi^+\pi^-$. This is estimated from the simulation that has been normalised to the 5 observed $J/\psi\psi(2S)$ events, where $\psi(2S) \rightarrow \mu^+\mu^-$. Only one of these events can be fully reconstructed and the invariant mass of one J/ψ meson and the two tracks, assumed to be pions, is consistent with that of the $\psi(2S)$ meson. The remainder of the distribution is uniform, suggestive of DPE events in which one or both protons dissociated. There is no indication of a contribution that increases towards higher multiplicities, as would be expected if there was a substantial contribution coming from non-exclusive events.

The selection of pairs of P-wave charmonia proceeds as for the S-wave, but the restriction on the number of photons is lifted. These criteria are only satisfied by two events. One event has a single photon and the invariant mass of a reconstructed J/ψ and this photon is consistent with the χ_{c0} mass; consequently, this event is a candidate for $\chi_{c0}\chi_{c0}$ production. The other event has two photons that, when combined, have the mass of a π^0 meson, and is thus not a candidate for $\chi_c\chi_c$ production. Both events are consistent with partially reconstructed $J/\psi\psi(2S)$ events where $\psi(2S) \rightarrow J/\psi\pi^0\pi^0$. Normalising to the five candidate events for $J/\psi\psi(2S)$, the simulation estimates that 2.8 ± 2.0 (0.5 ± 0.5) $J/\psi\psi(2S)$ events would be reconstructed as $J/\psi J/\psi$ candidates with one (two) additional photon(s). There are no candidates for $\chi_{c1}\chi_{c1}$ or $\chi_{c2}\chi_{c2}$ production.

4 Backgrounds

Three background components are considered: non-resonant background; feed-down from the exclusive production of other mesons; and inelastic production of mesons where one or both protons dissociate.

The non-resonant background is only considered for the S-wave analysis and is calculated by fitting an exponential to the non-signal contribution in Fig. 2 and extrapolating under the signal. It is estimated that there are 0.3 ± 0.1 and 0.07 ± 0.02 background events in the J/ψ and $\psi(2S)$ signal ranges, respectively.

A feed-down background is considered for the $J/\psi J/\psi$ and the P-wave analyses. Given the presence of five $J/\psi\psi(2S)$ signal events, it is expected that $\psi(2S) \rightarrow J/\psi X$ decays will occasionally be reconstructed as χ_c mesons or J/ψ mesons alone, due to the rest of the decay products being outside the acceptance or below threshold. Normalising to the five candidate events for $J/\psi\psi(2S)$, the simulation estimates that 2.9 ± 2.0 $J/\psi\psi(2S)$ events would be reconstructed as $J/\psi J/\psi$ candidates with no additional photons, while 0.8 ± 0.8 , 0.2 ± 0.2 and 0.1 ± 0.1 would be reconstructed as χ_{c0} , χ_{c1} and χ_{c2} mesons, respectively.

Feed-down from pairs of P-wave charmonia to give $J/\psi J/\psi$ candidates is also possible. The simulation estimates that in over 80% (70%) of $\chi_{c1}\chi_{c1}$ or $\chi_{c2}\chi_{c2}$ ($\chi_{c0}\chi_{c0}$) decays producing two J/ψ mesons, one or more additional photons would be detected. There is only one candidate for $\chi_{c0}\chi_{c0}$ but this is also consistent with feed-down from $J/\psi\psi(2S)$ events. Consequently, there is no evidence for a significant χ_c feed-down to the $J/\psi J/\psi$

selection and this contribution is assumed to be negligible.

The separation of the samples into those events that are truly exclusive (elastic) and those where one or both protons dissociate (inelastic) is fraught with difficulty. Therefore, the cross-sections are quoted for the full samples that are observed to be exclusively produced inside the LHCb acceptance, *i.e.* no other tracks or electromagnetic deposits are found in the detector. Nonetheless, to compare with theoretical predictions that are usually quoted for the elastic process without proton break-up, an attempt is made to quantify the elastic fraction in the $J/\psi J/\psi$ sample, using the distribution of squared transverse momentum and describing the elastic and proton-dissociation components by different exponential functions. This functional form is suggested by Regge theory that assumes the differential cross-section $d\sigma/dt \propto \exp(bt)$ for a wide class of diffractive events, where b is a constant for a given process, $t \approx -p_{T(p)}^2$ is the four-momentum transfer squared at one of the proton-pomeron vertices, and $p_{T(p)}$ is the transverse momentum of the outgoing proton labelled (p).

In the CEP single J/ψ analysis performed by the LHCb collaboration [2], the transverse momentum of the central system, $p_T \approx p_{T(p)}$, the transverse momentum of the outgoing proton from which the pomeron radiated. A fit to the p_T^2 distribution showed that the elastic contribution could be described by $d\sigma/dp_T^2 \sim \exp(-6 \text{ GeV}^{-2} p_T^2)$ and it was estimated that about 60% of events with $p_T^2 < 1 \text{ GeV}^2$ (corresponding to 40% of events without a requirement on p_T) were elastic.

In the CEP of pairs of J/ψ mesons, the situation should be similar, although $d\sigma/dp_T^2$ will fall off more gradually as there are two proton-pomeron vertices to consider. In addition, the dissociative background might be larger as the mass of the central system is higher and the production process is through two pomerons, rather than a photon and a pomeron. The transverse momentum of the central system, $p_T^2 = p_{T(p1)}^2 + p_{T(p2)}^2 + 2\vec{p}_{T(p1)} \cdot \vec{p}_{T(p2)}$. Taking a dependence of $\exp(-6 \text{ GeV}^{-2} p_{T(p)}^2)$ at each of the proton-pomeron vertices and ignoring possible rescattering effects leads to an expectation of $d\sigma/dp_T^2 \sim \exp(-3 \text{ GeV}^{-2} p_T^2)$. The p_T^2 distribution for the $J/\psi J/\psi$ candidates is shown in the left plot of Fig. 5 and has a

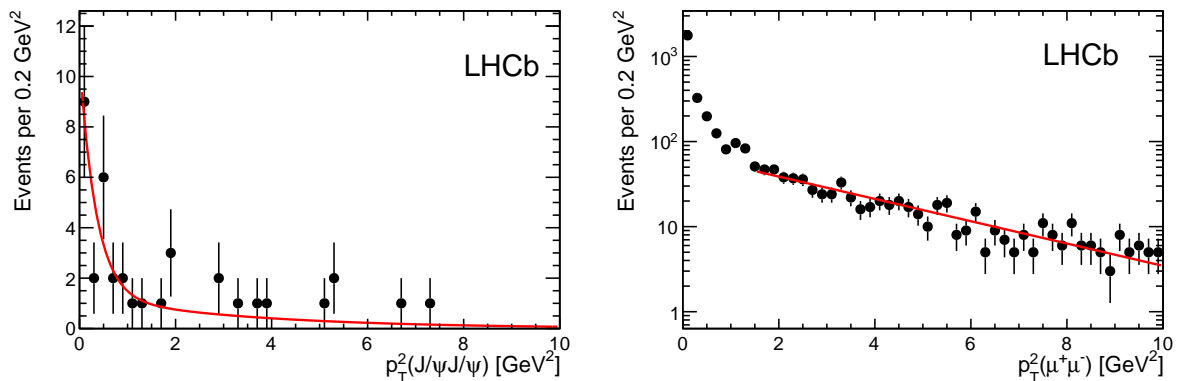


Figure 5: Transverse momentum squared distribution of candidates for exclusively produced (left) $J/\psi J/\psi$ and (right) dimuons whose invariant mass is between 6 and 9 GeV. The curves are fits to the data as described in the text.

shape similar to that seen in the exclusive J/ψ analyses: a peaking of signal events below 1 GeV^2 , and a tail to higher values, characteristic of inelastic production. A maximum likelihood fit is performed to the sum of two exponentials,

$$f_{\text{el}} b_s \exp(-b_s p_{\text{T}}^2) + (1 - f_{\text{el}}) b_b \exp(-b_b p_{\text{T}}^2), \quad (1)$$

where b_s, b_b are the slopes for the signal and background and f_{el} is the fraction of elastic events.

Due to the small sample size, the value of b_b is constrained using the distribution for exclusive dimuon candidates whose invariant mass lies in the range 6 to 9 GeV. These are selected as in the single J/ψ analysis [2] but with a different invariant mass requirement. The p_{T}^2 distribution, shown in the right plot of Fig. 5, has a prominent peak in the first bin corresponding to the electromagnetic two-photon exchange process, $pp \rightarrow p\mu^+\mu^-p$. The tail to larger values is characteristic of events with proton dissociation. The region $1.5 < p_{\text{T}}^2 < 10 \text{ GeV}^2$ is fit with a single exponential, resulting in a slope of $b_b = 0.29 \pm 0.02 \text{ GeV}^{-2}$.

Fixing b_b at this value of 0.29 GeV^{-2} , the fit to the p_{T}^2 distribution for the $J/\psi J/\psi$ candidates returns values of $b_s = 2.9 \pm 1.3 \text{ GeV}^{-2}$ and $f_{\text{el}} = 0.42 \pm 0.13$. An alternative fit is made with all parameters free, returning consistent results, albeit with larger uncertainties: $b_s = 3.1 \pm 1.7 \text{ GeV}^{-2}$, $b_b = 0.34 \pm 0.14 \text{ GeV}^{-2}$, $f_{\text{el}} = 0.38 \pm 0.17$. It is also worth noting that the p_{T}^2 spectrum of these selected events is different to that of inclusively selected J/ψ pairs, which can be fit with a single exponential with a slope of $0.051 \pm 0.001 \text{ GeV}^{-2}$.

5 Efficiency and acceptance

For dimesons in the rapidity range $2.0 < y < 4.5$, the acceptance factor, A , defines the fraction of events having four reconstructed tracks in the LHCb detector. This is found using simulated events that have been generated with a smoothed form of the distribution given in the left plot of Fig. 3, a p_{T}^2 as given in the left plot of Fig. 5, and a rapidity distribution according to the Durham model, which in the region $2.0 < y < 4.5$, can be described by the functional form $(1 - 0.18y)$.

To estimate a systematic uncertainty on the acceptance, the simulated events are reweighted with different assumptions on the mass, transverse momentum and rapidity of the dimeson system. The mass is described instead by the theoretical shape of Ref. [7], which changes the acceptance by less than 1%. The transverse momentum is described with the elastic shape found in data for the exclusive single J/ψ analysis [2], changing the acceptance by less than 1%. The largest effect is due to the assumption on the underlying rapidity distribution. An alternative model is to consider the pomeron as an isoscalar photon [29] and construct the pomeron flux from the Weizsäcker-Williams approximation for describing photon radiation. This leads to a rapidity distribution that is approximately flat for $2.0 < y < 4.5$ and an acceptance that changes by 6%.

The tracking efficiency also contributes to A . A systematic uncertainty of 1% per track has been determined [30] for tracks with pseudorapidities between 2.0 and 4.5. Uncertainties in the description of edge effects of the tracking detectors in the simulation

are assessed by comparing the pseudorapidity distributions of tracks in exclusive J/ψ events [2] in simulation and data. Differences are propagated to give an uncertainty on the determination of A for charmonium pairs of 7%. Combining all these effects in quadrature leads to estimates of 0.35 ± 0.03 for the acceptance of $J/\psi J/\psi$ events, 0.36 ± 0.03 for the acceptance of $J/\psi \psi(2S)$ and $\psi(2S)\psi(2S)$ events, and 0.29 ± 0.03 for the acceptance of any of the $\chi_c\chi_c$ pairs.

The efficiency, ϵ , for triggering and reconstructing signal events is the product of three quantities: $\epsilon_{\text{trigger}}$, ϵ_{muid} and ϵ_{sel} . The trigger only requires two of the four muons and consequently has a high efficiency of $\epsilon_{\text{trigger}} = 0.90 \pm 0.03$. This has been calculated from the single muon trigger efficiencies calculated in Ref. [2] together with the efficiency for the SPD multiplicity to be less than ten, which has been assessed using a rate-limited trigger that does not have requirements on the SPD multiplicity. The efficiency to identify three or more of the final-state decay products as muons, ϵ_{muid} , is high and the uncertainty is determined by propagating the difference in single muon efficiencies found in simulation and in data to give $\epsilon_{\text{muid}} = 0.95 \pm 0.03$. For the S-wave analysis, the selection has an efficiency $\epsilon_{\text{sel}} = 0.93 \pm 0.02$, which includes contributions from the requirements that no photons be identified in the event and that the reconstructed masses be within -200 MeV and $+65$ MeV of the J/ψ or $\psi(2S)$ mass. The former is found from simulation, calibrated using a sample of $J/\psi\gamma$ candidates in data, while the latter is determined from a fit to the peak in the exclusive J/ψ analysis [2]. For the P-wave analysis, the requirement of detecting one or more photons lowers the selection efficiency and values of $\epsilon_{\text{sel}} = 0.68 \pm 0.07, 0.77 \pm 0.04, 0.81 \pm 0.04$ are obtained for $\chi_{c0}\chi_{c0}, \chi_{c1}\chi_{c1}, \chi_{c2}\chi_{c2}$, respectively, where the uncertainty takes into account the modelling of the energy response of the calorimeter.

6 Results and discussion

The cross-section, $\sigma^{M_1M_2}$, for the production of meson pairs, M_1 and M_2 , is given by

$$\sigma^{M_1M_2} = \frac{N_{M_1M_2} - N_{\text{bkg}}}{(f_{\text{single}}L) A \epsilon \mathcal{B}(M_1 \rightarrow \mu\mu(\gamma)) \mathcal{B}(M_2 \rightarrow \mu\mu(\gamma))} \quad (2)$$

where $N_{M_1M_2}$ is the number of candidate meson pairs selected, N_{bkg} is the estimated number of background events, L is the integrated luminosity, f_{single} is the fraction of beam crossings with a single interaction, and $\mathcal{B}(M_i \rightarrow \mu\mu(\gamma))$ is the branching fraction for the meson to decay to two muons in the case of S-wave states, and two muons and a photon for P-wave states.

The luminosity has been determined with an uncertainty of 3.5% [31]. The factor, f_{single} , accounts for the fact that the selection requirements reject signal events that are accompanied by a visible proton-proton interaction in the same beam crossing, and is calculated as described in Ref. [2]. The cross-section measurements for 2011 and 2012 data are consistent and are combined to produce results at an average centre-of-mass energy of 7.6 TeV. All the numbers entering the cross-section calculation are given in

Table 1: Summary of numbers entering the cross-section calculation.

	$J/\psi J/\psi$	$J/\psi \psi(2S)$	$\psi(2S)\psi(2S)$	$\chi_{c0}\chi_{c0}$	$\chi_{c1}\chi_{c1}$	$\chi_{c2}\chi_{c2}$
$N_{M_1 M_2}$	37	5	0	1	0	0
N_{bkg}	3.2 ± 2.0	0.07 ± 0.02	< 0.01	0.8 ± 0.8	0.2 ± 0.2	0.1 ± 0.1
A	0.35 ± 0.03	0.36 ± 0.03	0.36 ± 0.03	0.29 ± 0.03	0.29 ± 0.03	0.29 ± 0.03
ϵ	0.80 ± 0.04	0.80 ± 0.04	0.80 ± 0.04	0.58 ± 0.06	0.66 ± 0.05	0.69 ± 0.05
$f_{\text{single}}L [\text{pb}^{-1}]$	596 ± 21					
$\mathcal{B}(J/\psi \rightarrow \mu\mu)$	0.0593 ± 0.0006					
$\mathcal{B}(\psi(2S) \rightarrow \mu\mu)$	0.0077 ± 0.0008					
$\mathcal{B}(\chi_{c0} \rightarrow J/\psi \gamma)$	0.0117 ± 0.0008					
$\mathcal{B}(\chi_{c1} \rightarrow J/\psi \gamma)$	0.344 ± 0.015					
$\mathcal{B}(\chi_{c2} \rightarrow J/\psi \gamma)$	0.195 ± 0.008					

Table 2: Percentage uncertainties on the quantities entering the denominator of Eq. (2).

Quantity	Relative size of systematic uncertainty [%]					
	$J/\psi J/\psi$	$J/\psi \psi(2S)$	$\psi(2S)\psi(2S)$	$\chi_{c0}\chi_{c0}$	$\chi_{c1}\chi_{c1}$	$\chi_{c2}\chi_{c2}$
A	9	9	9	9	9	9
ϵ	5	5	5	10	7	7
$f_{\text{single}}L [\text{pb}^{-1}]$	3.5	3.5	3.5	3.5	3.5	3.5
$\mathcal{B}(M_1)\mathcal{B}(M_2)$	2	10	21	14	8	9
Total	11	15	24	20	14	15

Table 1, while the systematic uncertainties of the quantities in the denominator of Eq. (2) are summarised in Table 2. Where zero or one candidate is observed, 90% confidence levels (CL) are calculated by performing pseudo-experiments in which the quantities in Eq. (2) are varied according to their uncertainties and pseudo-candidates are generated according to a Poisson distribution. The upper bound at 90% CL is defined as the smallest cross-section value that in 90% of pseudo-experiments leads to more candidate events than observed in data. The cross-sections, at an average energy of 7.6 TeV, for the dimeson system to be in the rapidity range $2.0 < y < 4.5$ with no other charged or neutral energy inside the LHCb acceptance are measured to be

$$\begin{aligned}
 \sigma^{J/\psi J/\psi} &= 58 \pm 10(\text{stat}) \pm 6(\text{syst}) \text{ pb}, \\
 \sigma^{J/\psi \psi(2S)} &= 63_{-18}^{+27}(\text{stat}) \pm 10(\text{syst}) \text{ pb}, \\
 \sigma^{\psi(2S)\psi(2S)} &< 237 \text{ pb}, \\
 \sigma^{\chi_{c0}\chi_{c0}} &< 69 \text{ nb}, \\
 \sigma^{\chi_{c1}\chi_{c1}} &< 45 \text{ pb}, \\
 \sigma^{\chi_{c2}\chi_{c2}} &< 141 \text{ pb},
 \end{aligned}$$

where the upper limits are at 90% CL. To compare with theory, the elastic fraction is taken

to be 0.42 ± 0.13 , as determined in Sec. 4, to give an estimated cross-section for central exclusive production of $J/\psi J/\psi$ of 24 ± 9 pb, where all the uncertainties are combined in quadrature. Using the formalism of Ref. [12], a preliminary prediction [32] of 8 pb at $\sqrt{s} = 8$ TeV has been obtained. There is a large uncertainty of a factor two to three on this value due to the gluon parton density function that enters with the fourth power, the choice of the gap survival factor [33], and the value of the J/ψ wave-function at the origin [7, 11, 34]. Theory and experiment are observed to be in reasonable agreement, given the large uncertainties that currently exist on both.

The relative sizes of the cross-sections for exclusive $J/\psi \psi(2S)$ and $J/\psi J/\psi$ production, assuming a similar elastic fraction, is

$$\frac{\sigma(J/\psi \psi(2S))}{\sigma(J/\psi J/\psi)} = 1.1^{+0.5}_{-0.4},$$

where the total uncertainty is quoted and most systematics, bar that on the branching fractions, cancel in the ratio. This is in agreement with a theoretical estimate for this ratio of about 0.5 [7]. The equivalent quantity measured in exclusive single charmonium production [2] is

$$\frac{\sigma(\psi(2S))}{\sigma(J/\psi)} = 0.17 \pm 0.02.$$

No strong conclusion can be drawn on the higher relative fraction of $\psi(2S)$ to J/ψ in double charmonium production compared to that in single charmonium production, due to the large uncertainty.

The ratios of double to single J/ψ production can be compared in the inclusive and exclusive modes. The inclusive ratio was measured by LHCb [8] to be

$$\sigma^{J/\psi J/\psi} / \sigma^{J/\psi} |_{\text{inclusive}} = (5.1 \pm 1.0 \pm 0.6^{+1.2}_{-1.0}) \times 10^{-4}.$$

The exclusive single J/ψ cross-section is calculated from the differential cross-section and acceptance values given in Tables 2 and 3 of Ref. [2] and the branching fraction to dimuons to get $\sigma^{J/\psi} = 11.2 \pm 0.8$ nb. A combination with the estimated exclusive elastic cross-section above gives

$$\sigma^{J/\psi J/\psi} / \sigma^{J/\psi} |_{\text{exclusive}} = (2.1 \pm 0.8) \times 10^{-3},$$

the central value for which is four times higher than in the inclusive case, though again, due to the large uncertainty, both are consistent.

7 Conclusions

A clear signal for the production of pairs of S-wave charmonia in the absence of other activity in the LHCb acceptance is obtained. This is the first observation of the central exclusive production of pairs of charmonia. The small sample size affects the precision with which the elastic component can be extracted. A fit to the p_{T}^2 of the system of two

J/ψ mesons estimates that $(42 \pm 13)\%$ of the events that are observed to be exclusive in the LHCb detector is elastically produced while the remainder is attributed to events in which one or both protons dissociate. The measurement are in agreement with preliminary theoretical predictions. No signal is observed for the production of pairs of P-wave charmonia and upper limits on the cross-sections are set.

Acknowledgements

We thank Lucian Harland-Lang and Valery Khoze for many helpful discussions and for providing theoretical predictions. We express our gratitude to our colleagues in the CERN accelerator departments for the excellent performance of the LHC. We thank the technical and administrative staff at the LHCb institutes. We acknowledge support from CERN and from the national agencies: CAPES, CNPq, FAPERJ and FINEP (Brazil); NSFC (China); CNRS/IN2P3 (France); BMBF, DFG, HGF and MPG (Germany); SFI (Ireland); INFN (Italy); FOM and NWO (The Netherlands); MNiSW and NCN (Poland); MEN/IFA (Romania); MinES and FANO (Russia); MinECo (Spain); SNSF and SER (Switzerland); NASU (Ukraine); STFC (United Kingdom); NSF (USA). The Tier1 computing centres are supported by IN2P3 (France), KIT and BMBF (Germany), INFN (Italy), NWO and SURF (The Netherlands), PIC (Spain), GridPP (United Kingdom). We are indebted to the communities behind the multiple open source software packages on which we depend. We are also thankful for the computing resources and the access to software R&D tools provided by Yandex LLC (Russia). Individual groups or members have received support from EPLANET, Marie Skłodowska-Curie Actions and ERC (European Union), Conseil général de Haute-Savoie, Labex ENIGMASS and OCEVU, Région Auvergne (France), RFBR (Russia), XuntaGal and GENCAT (Spain), Royal Society and Royal Commission for the Exhibition of 1851 (United Kingdom).

References

- [1] M. G. Albrow, T. D. Coughlin, and J. R. Forshaw, *Central exclusive particle production at high energy hadron colliders*, Prog. Part. Nucl. Phys. **65** (2010) 149, [arXiv:1006.1289](#).
- [2] LHCb collaboration, R. Aaij *et al.*, *Updated measurements of exclusive J/ψ and $\psi(2S)$ production cross-sections in pp collisions at $\sqrt{s} = 7$ TeV*, J. Phys. **G41** (2014) 055002, [arXiv:1401.3288](#).
- [3] ALICE collaboration, B. B. Abelev *et al.*, *Exclusive J/ψ photoproduction off protons in ultra-peripheral p -Pb collisions at $\sqrt{s_{NN}}=5.02$ TeV*, [arXiv:1406.7819](#).
- [4] WA102 collaboration, D. Barberis *et al.*, *A study of the $\omega\omega$ channel produced in central pp interactions at 450 GeV/c*, Phys. Lett. **B484** (2000) 198, [arXiv:hep-ex/0005027](#).

- [5] WA102 Collaboration, D. Barberis *et al.*, *A study of the centrally produced $\phi\phi$ system in pp interactions at $450\text{ GeV}/c$* , Phys. Lett. **B432** (1998) 436, [arXiv:hep-ex/9805018](#).
- [6] WA76 collaboration, T. A. Armstrong *et al.*, *Observation of double ϕ meson production in the central region for the reaction $pp \rightarrow p_f(K^+K^-K^+K^-)p_s$ at $300\text{-GeV}/c$* , Phys. Lett. **B221** (1989) 221.
- [7] A. V. Berezhnoy, A. K. Likhoded, A. V. Luchinsky, and A. A. Novoselov, *Double J/ψ -meson production at LHC and $4c$ -tetraquark state*, Phys. Rev. **D84** (2011) 094023, [arXiv:1101.5881](#).
- [8] LHCb collaboration, R. Aaij *et al.*, *Observation of J/ψ pair production in pp collisions at $\sqrt{s} = 7\text{ TeV}$* , Phys. Lett. **B707** (2012) 52, [arXiv:1109.0963](#).
- [9] J. R. Gaunt, C. H. Kom, A. Kulesza, and W. J. Stirling, *Probing double parton scattering with leptonic final states at the LHC*, [arXiv:1110.1174](#).
- [10] L. A. Harland-Lang, V. A. Khoze, M. G. Ryskin, and W. J. Stirling, *Central exclusive production within the Durham model: a review*, Int. J. Mod. Phys. **A29** (2014) 1430031, [arXiv:1405.0018](#).
- [11] C.-F. Qiao, L.-P. Sun, and P. Sun, *Testing charmonium production mechanism via polarized J/ψ pair production at the LHC*, J. Phys. **G37** (2010) 075019, [arXiv:0903.0954](#).
- [12] L. A. Harland-Lang, V. A. Khoze, M. G. Ryskin, and W. J. Stirling, *Central exclusive meson pair production in the perturbative regime at hadron colliders*, Eur. Phys. J. **C71** (2011) 1714, [arXiv:1105.1626](#).
- [13] S. L. Grayson, R. R. Horgan, and P. V. Landshoff, *Exclusive production of heavy mesons in photon-photon collisions: the double scattering mechanism*, Z. Phys. **C20** (1983) 43.
- [14] I. F. Ginzburg, S. L. Panfil, and V. G. Serbo, *The semihard processes $\gamma\gamma \rightarrow \psi X$, $\gamma\gamma \rightarrow \psi\psi$, $\gamma\gamma \rightarrow \rho\psi$* , Nucl. Phys. **B296** (1988) 569.
- [15] C.-F. Qiao, *Double J/ψ production at photon colliders*, Phys. Rev. **D64** (2001) 077503, [arXiv:hep-ph/0104309](#).
- [16] V. P. Gonçalves and M. V. T. Machado, *The QCD pomeron in ultraperipheral heavy ion collisions. 1. The Double J/ψ production*, Eur. Phys. J. **C28** (2003) 71, [arXiv:hep-ph/0212178](#).
- [17] A. Cisek, W. Schäfer, and A. Szczurek, *Exclusive coherent production of heavy vector mesons in nucleus-nucleus collisions at energies available at the CERN Large Hadron Collider*, Phys. Rev. **C86** (2012) 014905, [arXiv:1204.5381](#).

- [18] S. Baranov *et al.*, *The $\gamma\gamma \rightarrow J/\psi J/\psi$ reaction and the $J/\psi J/\psi$ pair production in exclusive ultraperipheral ultrarelativistic heavy ion collisions*, Eur. Phys. J. **C73** (2013) 2335, [arXiv:1208.5917](#).
- [19] L. A. Harland-Lang, V. A. Khoze, M. G. Ryskin, and W. J. Stirling, *Central exclusive χ_c meson production at the Tevatron revisited*, Eur. Phys. J. **C65** (2010) 433, [arXiv:0909.4748](#).
- [20] LHCb collaboration, A. A. Alves Jr. *et al.*, *The LHCb detector at the LHC*, JINST **3** (2008) S08005.
- [21] R. Aaij *et al.*, *Performance of the LHCb Vertex Locator*, JINST **9** (2014) 09007, [arXiv:1405.7808](#).
- [22] LHCb Outer Tracker group, R. Arink *et al.*, *Performance of the LHCb Outer Tracker*, JINST **9** (2014) 01002, [arXiv:1311.3893](#).
- [23] M. Adinolfi *et al.*, *Performance of the LHCb RICH detector at the LHC*, Eur. Phys. J. **C73** (2013) 2431, [arXiv:1211.6759](#).
- [24] A. A. Alves Jr. *et al.*, *Performance of the LHCb muon system*, JINST **8** (2013) P02022, [arXiv:1211.1346](#).
- [25] R. Aaij *et al.*, *The LHCb trigger and its performance in 2011*, JINST **8** (2013) P04022, [arXiv:1211.3055](#).
- [26] T. Sjöstrand, S. Mrenna, and P. Skands, *PYTHIA 6.4 physics and manual*, JHEP **05** (2006) 026, [arXiv:hep-ph/0603175](#).
- [27] Geant4 collaboration, S. Agostinelli *et al.*, *Geant4: a simulation toolkit*, Nucl. Instrum. Meth. **A506** (2003) 250.
- [28] Particle Data Group, J. Beringer *et al.*, *Review of particle physics*, Phys. Rev. **D86** (2012) 010001, and 2013 partial update for the 2014 edition.
- [29] A. Donnachie and P. V. Landshoff, *Hard diffraction: production of high p_T jets, W or Z , and Drell-Yan pairs*, Nucl. Phys. **B303** (1988) 634.
- [30] A. Jaeger *et al.*, *Measurement of the track finding efficiency*, LHCb-PUB-2011-025.
- [31] LHCb collaboration, R. Aaij *et al.*, *Absolute luminosity measurements with the LHCb detector at the LHC*, JINST **7** (2012) P01010, [arXiv:1110.2866](#).
- [32] L. A. Harland-Lang, V. A. Khoze, and M. G. Ryskin, *Private communication*, Publication in preparation.
- [33] V. A. Khoze, A. D. Martin, and M. G. Ryskin, *Diffraction at the LHC*, Eur. Phys. J. **C73** (2013) 2503, [arXiv:1306.2149](#).

- [34] G. T. Bodwin, E. Braaten, and G. P. Lepage, *Rigorous QCD analysis of inclusive annihilation and production of heavy quarkonium*, Phys. Rev. **D51** (1995) 1125, arXiv:hep-ph/9407339.

LHCb collaboration

R. Aaij⁴¹, B. Adeva³⁷, M. Adinolfi⁴⁶, A. Affolder⁵², Z. Ajaltouni⁵, S. Akar⁶, J. Albrecht⁹, F. Alessio³⁸, M. Alexander⁵¹, S. Ali⁴¹, G. Alkhazov³⁰, P. Alvarez Cartelle³⁷, A.A. Alves Jr^{25,38}, S. Amato², S. Amerio²², Y. Amhis⁷, L. An³, L. Anderlini^{17,g}, J. Anderson⁴⁰, R. Andreassen⁵⁷, M. Andreotti^{16,f}, J.E. Andrews⁵⁸, R.B. Appleby⁵⁴, O. Aquines Gutierrez¹⁰, F. Archilli³⁸, A. Artamonov³⁵, M. Artuso⁵⁹, E. Aslanides⁶, G. Auriemma^{25,n}, M. Baalouch⁵, S. Bachmann¹¹, J.J. Back⁴⁸, A. Badalov³⁶, W. Baldini¹⁶, R.J. Barlow⁵⁴, C. Barschel³⁸, S. Barsuk⁷, W. Barter⁴⁷, V. Batozskaya²⁸, V. Battista³⁹, A. Bay³⁹, L. Beaucourt⁴, J. Beddow⁵¹, F. Bedeschi²³, I. Bediaga¹, S. Belogurov³¹, K. Belous³⁵, I. Belyaev³¹, E. Ben-Haim⁸, G. Bencivenni¹⁸, S. Benson³⁸, J. Benton⁴⁶, A. Berezhnoy³², R. Bernet⁴⁰, M.-O. Bettler⁴⁷, M. van Beuzekom⁴¹, A. Bien¹¹, S. Bifani⁴⁵, T. Bird⁵⁴, A. Bizzeti^{17,i}, P.M. Bjørnstad⁵⁴, T. Blake⁴⁸, F. Blanc³⁹, J. Blouw¹⁰, S. Blusk⁵⁹, V. Bocci²⁵, A. Bondar³⁴, N. Bondar^{30,38}, W. Bonivento^{15,38}, S. Borghi⁵⁴, A. Borgia⁵⁹, M. Borsato⁷, T.J.V. Bowcock⁵², E. Bowen⁴⁰, C. Bozzi¹⁶, T. Brambach⁹, J. van den Brand⁴², J. Bressieux³⁹, D. Brett⁵⁴, M. Britsch¹⁰, T. Britton⁵⁹, J. Brodzicka⁵⁴, N.H. Brook⁴⁶, H. Brown⁵², A. Bursche⁴⁰, G. Busetto^{22,r}, J. Buytaert³⁸, S. Cadeddu¹⁵, R. Calabrese^{16,f}, M. Calvi^{20,k}, M. Calvo Gomez^{36,p}, P. Campana^{18,38}, D. Campora Perez³⁸, A. Carbone^{14,d}, G. Carboni^{24,l}, R. Cardinale^{19,38,j}, A. Cardini¹⁵, L. Carson⁵⁰, K. Carvalho Akiba², G. Casse⁵², L. Cassina²⁰, L. Castillo Garcia³⁸, M. Cattaneo³⁸, Ch. Cauet⁹, R. Cenci⁵⁸, M. Charles⁸, Ph. Charpentier³⁸, M. Chefdeville⁴, S. Chen⁵⁴, S.-F. Cheung⁵⁵, N. Chiapolini⁴⁰, M. Chrzaszcz^{40,26}, K. Ciba³⁸, X. Cid Vidal³⁸, G. Ciezarek⁵³, P.E.L. Clarke⁵⁰, M. Clemencic³⁸, H.V. Cliff⁴⁷, J. Closier³⁸, V. Coco³⁸, J. Cogan⁶, E. Cogneras⁵, L. Cojocariu²⁹, P. Collins³⁸, A. Comerma-Montells¹¹, A. Contu¹⁵, A. Cook⁴⁶, M. Coombes⁴⁶, S. Coquereau⁸, G. Corti³⁸, M. Corvo^{16,f}, I. Counts⁵⁶, B. Couturier³⁸, G.A. Cowan⁵⁰, D.C. Craik⁴⁸, M. Cruz Torres⁶⁰, S. Cunliffe⁵³, R. Currie⁵⁰, C. D'Ambrosio³⁸, J. Dalseno⁴⁶, P. David⁸, P.N.Y. David⁴¹, A. Davis⁵⁷, K. De Bruyn⁴¹, S. De Capua⁵⁴, M. De Cian¹¹, J.M. De Miranda¹, L. De Paula², W. De Silva⁵⁷, P. De Simone¹⁸, D. Decamp⁴, M. Deckenhoff⁹, L. Del Buono⁸, N. Déléage⁴, D. Derkach⁵⁵, O. Deschamps⁵, F. Dettori³⁸, A. Di Canto³⁸, H. Dijkstra³⁸, S. Donleavy⁵², F. Dordei¹¹, M. Dorigo³⁹, A. Dosil Suárez³⁷, D. Dossett⁴⁸, A. Dovbnya⁴³, K. Dreimanis⁵², G. Dujany⁵⁴, F. Dupertuis³⁹, P. Durante³⁸, R. Dzhelyadin³⁵, A. Dziurda²⁶, A. Dzyuba³⁰, S. Easo^{49,38}, U. Egede⁵³, V. Egorychev³¹, S. Eidelman³⁴, S. Eisenhardt⁵⁰, U. Eitschberger⁹, R. Ekelhof⁹, L. Eklund⁵¹, I. El Rifai⁵, Ch. Elsasser⁴⁰, S. Ely⁵⁹, S. Esen¹¹, H.-M. Evans⁴⁷, T. Evans⁵⁵, A. Falabella¹⁴, C. Färber¹¹, C. Farinelli⁴¹, N. Farley⁴⁵, S. Farry⁵², R.F. Fay⁵², D. Ferguson⁵⁰, V. Fernandez Albor³⁷, F. Ferreira Rodrigues¹, M. Ferro-Luzzi³⁸, S. Filippov³³, M. Fiore^{16,f}, M. Fiorini^{16,f}, M. Firlej²⁷, C. Fitzpatrick³⁹, T. Fiutowski²⁷, M. Fontana¹⁰, F. Fontanelli^{19,j}, R. Forty³⁸, O. Francisco², M. Frank³⁸, C. Frei³⁸, M. Frosini^{17,38,g}, J. Fu^{21,38}, E. Furfaro^{24,l}, A. Gallas Torreira³⁷, D. Galli^{14,d}, S. Gallorini²², S. Gambetta^{19,j}, M. Gandelman², P. Gandini⁵⁹, Y. Gao³, J. García Pardiñas³⁷, J. Garofoli⁵⁹, J. Garra Tico⁴⁷, L. Garrido³⁶, C. Gaspar³⁸, R. Gauld⁵⁵, L. Gavardi⁹, G. Gavrillov³⁰, A. Geraci^{21,v}, E. Gersabeck¹¹, M. Gersabeck⁵⁴, T. Gershon⁴⁸, Ph. Ghez⁴, A. Gianelle²², S. Giani³⁹, V. Gibson⁴⁷, L. Giubega²⁹, V.V. Gligorov³⁸, C. Göbel⁶⁰, D. Golubkov³¹, A. Golutvin^{53,31,38}, A. Gomes^{1,a}, C. Gotti²⁰, M. Grabalosa Gándara⁵, R. Graciani Diaz³⁶, L.A. Granado Cardoso³⁸, E. Graugés³⁶, G. Graziani¹⁷, A. Grecu²⁹, E. Greening⁵⁵, S. Gregson⁴⁷, P. Griffith⁴⁵, L. Grillo¹¹, O. Grünberg⁶², B. Gui⁵⁹, E. Gushchin³³, Yu. Guz^{35,38}, T. Gys³⁸, C. Hadjivasiliou⁵⁹, G. Haefeli³⁹, C. Haen³⁸, S.C. Haines⁴⁷, S. Hall⁵³, B. Hamilton⁵⁸, T. Hampson⁴⁶, X. Han¹¹, S. Hansmann-Menzemer¹¹, N. Harnew⁵⁵, S.T. Harnew⁴⁶, J. Harrison⁵⁴,

J. He³⁸, T. Head³⁸, V. Heijne⁴¹, K. Hennessy⁵², P. Henrard⁵, L. Henry⁸,
 J.A. Hernando Morata³⁷, E. van Herwijnen³⁸, M. Heß⁶², A. Hicheur¹, D. Hill⁵⁵, M. Hoballah⁵,
 C. Hombach⁵⁴, W. Hulsbergen⁴¹, P. Hunt⁵⁵, N. Hussain⁵⁵, D. Hutchcroft⁵², D. Hynds⁵¹,
 M. Idzik²⁷, P. Ilten⁵⁶, R. Jacobsson³⁸, A. Jaeger¹¹, J. Jalocha⁵⁵, E. Jans⁴¹, P. Jatón³⁹,
 A. Jawahery⁵⁸, F. Jing³, M. John⁵⁵, D. Johnson⁵⁵, C.R. Jones⁴⁷, C. Joram³⁸, B. Jost³⁸,
 N. Jurik⁵⁹, M. Kabbalo⁹, S. Kandybei⁴³, W. Kanso⁶, M. Karacson³⁸, T.M. Karbach³⁸,
 S. Karodia⁵¹, M. Kelsey⁵⁹, I.R. Kenyon⁴⁵, T. Ketel⁴², B. Khanji²⁰, C. Khurewathanakul³⁹,
 S. Klaver⁵⁴, K. Klimaszewski²⁸, O. Kochebina⁷, M. Kolpin¹¹, I. Komarov³⁹, R.F. Koopman⁴²,
 P. Koppenburg^{41,38}, M. Korolev³², A. Kozlinskiy⁴¹, L. Kravchuk³³, K. Kreplin¹¹, M. Krepis⁴⁸,
 G. Krocker¹¹, P. Krokovny³⁴, F. Kruse⁹, W. Kucewicz^{26,o}, M. Kucharczyk^{20,26,38,k},
 V. Kudryavtsev³⁴, K. Kurek²⁸, T. Kvaratskheliya³¹, V.N. La Thi³⁹, D. Lacarrere³⁸,
 G. Lafferty⁵⁴, A. Lai¹⁵, D. Lambert⁵⁰, R.W. Lambert⁴², G. Lanfranchi¹⁸, C. Langenbruch⁴⁸,
 B. Langhans³⁸, T. Latham⁴⁸, C. Lazzeroni⁴⁵, R. Le Gac⁶, J. van Leerdam⁴¹, J.-P. Lees⁴,
 R. Lefèvre⁵, A. Leflat³², J. Lefrançois⁷, S. Leo²³, O. Leroy⁶, T. Lesiak²⁶, B. Leverington¹¹,
 Y. Li³, T. Likhomanenko⁶³, M. Liles⁵², R. Lindner³⁸, C. Linn³⁸, F. Lionetto⁴⁰, B. Liu¹⁵,
 S. Lohn³⁸, I. Longstaff⁵¹, J.H. Lopes², N. Lopez-March³⁹, P. Lowdon⁴⁰, H. Lu³, D. Lucchesi^{22,r},
 H. Luo⁵⁰, A. Lupato²², E. Luppi^{16,f}, O. Lupton⁵⁵, F. Machefert⁷, I.V. Machikhiliyan³¹,
 F. Maciuc²⁹, O. Maev³⁰, S. Malde⁵⁵, A. Malinin⁶³, G. Manca^{15,e}, G. Mancinelli⁶, A. Mapelli³⁸,
 J. Maratas⁵, J.F. Marchand⁴, U. Marconi¹⁴, C. Marin Benito³⁶, P. Marino^{23,t}, R. Märki³⁹,
 J. Marks¹¹, G. Martellotti²⁵, A. Martens⁸, A. Martín Sánchez⁷, M. Martinelli³⁹,
 D. Martinez Santos⁴², F. Martinez Vidal⁶⁴, D. Martins Tostes², A. Massafferri¹, R. Matev³⁸,
 Z. Mathe³⁸, C. Matteuzzi²⁰, A. Mazurov^{16,f}, M. McCann⁵³, J. McCarthy⁴⁵, A. McNab⁵⁴,
 R. McNulty¹², B. McSkelly⁵², B. Meadows⁵⁷, F. Meier⁹, M. Meissner¹¹, M. Merk⁴¹,
 D.A. Milanese⁸, M.-N. Minard⁴, N. Moggi¹⁴, J. Molina Rodriguez⁶⁰, S. Monteil⁵, M. Morandin²²,
 P. Morawski²⁷, A. Mordà⁶, M.J. Morello^{23,t}, J. Moron²⁷, A.-B. Morris⁵⁰, R. Mountain⁵⁹,
 F. Muheim⁵⁰, K. Müller⁴⁰, M. Mussini¹⁴, B. Muster³⁹, P. Naik⁴⁶, T. Nakada³⁹,
 R. Nandakumar⁴⁹, I. Nasteva², M. Needham⁵⁰, N. Neri²¹, S. Neubert³⁸, N. Neufeld³⁸,
 M. Neuner¹¹, A.D. Nguyen³⁹, T.D. Nguyen³⁹, C. Nguyen-Mau^{39,q}, M. Nicol⁷, V. Niess⁵,
 R. Niet⁹, N. Nikitin³², T. Nikodem¹¹, A. Novoselov³⁵, D.P. O'Hanlon⁴⁸, A. Oblakowska-Mucha²⁷,
 V. Obraztsov³⁵, S. Oggero⁴¹, S. Ogilvy⁵¹, O. Okhrimenko⁴⁴, R. Oldeman^{15,e}, G. Onderwater⁶⁵,
 M. Orlandea²⁹, B. Osorio Rodrigues¹, J.M. Otalora Goicochea², P. Owen⁵³, A. Oyanguren⁶⁴,
 B.K. Pal⁵⁹, A. Palano^{13,c}, F. Palombo^{21,u}, M. Palutan¹⁸, J. Panman³⁸, A. Papanestis^{49,38},
 M. Pappagallo⁵¹, L.L. Pappalardo^{16,f}, C. Parkes⁵⁴, C.J. Parkinson^{9,45}, G. Passaleva¹⁷,
 G.D. Patel⁵², M. Patel⁵³, C. Patrignani^{19,j}, A. Pazos Alvarez³⁷, A. Pearce⁵⁴, A. Pellegrino⁴¹,
 M. Pepe Altarelli³⁸, S. Perazzini^{14,d}, E. Perez Trigo³⁷, P. Perret⁵, M. Perrin-Terrin⁶,
 L. Pescatore⁴⁵, E. Pesen⁶⁶, K. Petridis⁵³, A. Petrolini^{19,j}, E. Picatoste Olloqui³⁶, B. Pietrzyk⁴,
 T. Pilař⁴⁸, D. Pinci²⁵, A. Pistone¹⁹, S. Playfer⁵⁰, M. Plo Casasus³⁷, F. Polci⁸, A. Poluektov^{48,34},
 E. Polcarpo², A. Popov³⁵, D. Popov¹⁰, B. Popovici²⁹, C. Potterat², E. Price⁴⁶,
 J. Prisciandaro³⁹, A. Pritchard⁵², C. Prouve⁴⁶, V. Pugatch⁴⁴, A. Puig Navarro³⁹, G. Punzi^{23,s},
 W. Qian⁴, B. Rachwal²⁶, J.H. Rademacker⁴⁶, B. Rakotomiamanana³⁹, M. Rama¹⁸,
 M.S. Rangel², I. Raniuk⁴³, N. Rauschmayr³⁸, G. Raven⁴², S. Reichert⁵⁴, M.M. Reid⁴⁸,
 A.C. dos Reis¹, S. Ricciardi⁴⁹, S. Richards⁴⁶, M. Rihl³⁸, K. Rinnert⁵², V. Rives Molina³⁶,
 D.A. Roa Romero⁵, P. Robbe⁷, A.B. Rodrigues¹, E. Rodrigues⁵⁴, P. Rodriguez Perez⁵⁴,
 S. Roiser³⁸, V. Romanovsky³⁵, A. Romero Vidal³⁷, M. Rotondo²², J. Rouvinet³⁹, T. Rul³⁸,
 H. Ruiz³⁶, P. Ruiz Valls⁶⁴, J.J. Saborido Silva³⁷, N. Sagidova³⁰, P. Sail⁵¹, B. Saitta^{15,e},
 V. Salustino Guimaraes², C. Sanchez Mayordomo⁶⁴, B. Sanmartin Sedes³⁷, R. Santacesaria²⁵,

C. Santamarina Rios³⁷, E. Santovetti^{24,l}, A. Sarti^{18,m}, C. Satriano^{25,n}, A. Satta²⁴,
D.M. Saunders⁴⁶, M. Savrie^{16,f}, D. Savrina^{31,32}, M. Schiller⁴², H. Schindler³⁸, M. Schlupp⁹,
M. Schmelling¹⁰, B. Schmidt³⁸, O. Schneider³⁹, A. Schopper³⁸, M.-H. Schune⁷, R. Schwemmer³⁸,
B. Sciascia¹⁸, A. Sciubba²⁵, M. Seco³⁷, A. Semennikov³¹, I. Sepp⁵³, N. Serra⁴⁰, J. Serrano⁶,
L. Sestini²², P. Seyfert¹¹, M. Shapkin³⁵, I. Shapoval^{16,43,f}, Y. Shcheglov³⁰, T. Shears⁵²,
L. Shekhtman³⁴, V. Shevchenko⁶³, A. Shires⁹, R. Silva Coutinho⁴⁸, G. Simi²², M. Sirendi⁴⁷,
N. Skidmore⁴⁶, T. Skwarnicki⁵⁹, N.A. Smith⁵², E. Smith^{55,49}, E. Smith⁵³, J. Smith⁴⁷,
M. Smith⁵⁴, H. Snoek⁴¹, M.D. Sokoloff⁵⁷, F.J.P. Soler⁵¹, F. Soomro³⁹, D. Souza⁴⁶,
B. Souza De Paula², B. Spaan⁹, A. Sparkes⁵⁰, P. Spradlin⁵¹, S. Sridharan³⁸, F. Stagni³⁸,
M. Stahl¹¹, S. Stahl¹¹, O. Steinkamp⁴⁰, O. Stenyakin³⁵, S. Stevenson⁵⁵, S. Stoica²⁹, S. Stone⁵⁹,
B. Storaci⁴⁰, S. Stracka^{23,38}, M. Straticiuc²⁹, U. Straumann⁴⁰, R. Stroili²², V.K. Subbiah³⁸,
L. Sun⁵⁷, W. Sutcliffe⁵³, K. Swientek²⁷, S. Swientek⁹, V. Syropoulos⁴², M. Szczekowski²⁸,
P. Szczypka^{39,38}, D. Szilard², T. Szumlak²⁷, S. T'Jampens⁴, M. Teklishyn⁷, G. Tellarini^{16,f},
F. Teubert³⁸, C. Thomas⁵⁵, E. Thomas³⁸, J. van Tilburg⁴¹, V. Tisserand⁴, M. Tobin³⁹,
S. Tolk⁴², L. Tomassetti^{16,f}, D. Tonelli³⁸, S. Topp-Joergensen⁵⁵, N. Torr⁵⁵, E. Tournefier⁴,
S. Tourneur³⁹, M.T. Tran³⁹, M. Tresch⁴⁰, A. Tsaregorodtsev⁶, P. Tsopelas⁴¹, N. Tuning⁴¹,
M. Ubeda Garcia³⁸, A. Ukleja²⁸, A. Ustyuzhanin⁶³, U. Uwer¹¹, V. Vagnoni¹⁴, G. Valenti¹⁴,
A. Vallier⁷, R. Vazquez Gomez¹⁸, P. Vazquez Regueiro³⁷, C. Vázquez Sierra³⁷, S. Vecchi¹⁶,
J.J. Velthuis⁴⁶, M. Veltri^{17,h}, G. Veneziano³⁹, M. Vesterinen¹¹, B. Viaud⁷, D. Vieira²,
M. Vieites Diaz³⁷, X. Vilasis-Cardona^{36,p}, A. Vollhardt⁴⁰, D. Volynskyy¹⁰, D. Voong⁴⁶,
A. Vorobyev³⁰, V. Vorobyev³⁴, C. Voß⁶², H. Voss¹⁰, J.A. de Vries⁴¹, R. Waldi⁶², C. Wallace⁴⁸,
R. Wallace¹², J. Walsh²³, S. Wandernoth¹¹, J. Wang⁵⁹, D.R. Ward⁴⁷, N.K. Watson⁴⁵,
D. Websdale⁵³, M. Whitehead⁴⁸, J. Wicht³⁸, D. Wiedner¹¹, G. Wilkinson⁵⁵, M.P. Williams⁴⁵,
M. Williams⁵⁶, F.F. Wilson⁴⁹, J. Wimberley⁵⁸, J. Wishahi⁹, W. Wislicki²⁸, M. Witek²⁶,
G. Wormser⁷, S.A. Wotton⁴⁷, S. Wright⁴⁷, S. Wu³, K. Wyllie³⁸, Y. Xie⁶¹, Z. Xing⁵⁹, Z. Xu³⁹,
Z. Yang³, X. Yuan³, O. Yushchenko³⁵, M. Zangoli¹⁴, M. Zavertyaev^{10,b}, L. Zhang⁵⁹,
W.C. Zhang¹², Y. Zhang³, A. Zhelezov¹¹, A. Zhokhov³¹, L. Zhong³, A. Zvyagin³⁸.

¹ Centro Brasileiro de Pesquisas Físicas (CBPF), Rio de Janeiro, Brazil

² Universidade Federal do Rio de Janeiro (UFRJ), Rio de Janeiro, Brazil

³ Center for High Energy Physics, Tsinghua University, Beijing, China

⁴ LAPP, Université de Savoie, CNRS/IN2P3, Annecy-Le-Vieux, France

⁵ Clermont Université, Université Blaise Pascal, CNRS/IN2P3, LPC, Clermont-Ferrand, France

⁶ CPPM, Aix-Marseille Université, CNRS/IN2P3, Marseille, France

⁷ LAL, Université Paris-Sud, CNRS/IN2P3, Orsay, France

⁸ LPNHE, Université Pierre et Marie Curie, Université Paris Diderot, CNRS/IN2P3, Paris, France

⁹ Fakultät Physik, Technische Universität Dortmund, Dortmund, Germany

¹⁰ Max-Planck-Institut für Kernphysik (MPIK), Heidelberg, Germany

¹¹ Physikalisches Institut, Ruprecht-Karls-Universität Heidelberg, Heidelberg, Germany

¹² School of Physics, University College Dublin, Dublin, Ireland

¹³ Sezione INFN di Bari, Bari, Italy

¹⁴ Sezione INFN di Bologna, Bologna, Italy

¹⁵ Sezione INFN di Cagliari, Cagliari, Italy

¹⁶ Sezione INFN di Ferrara, Ferrara, Italy

¹⁷ Sezione INFN di Firenze, Firenze, Italy

¹⁸ Laboratori Nazionali dell'INFN di Frascati, Frascati, Italy

¹⁹ Sezione INFN di Genova, Genova, Italy

²⁰ Sezione INFN di Milano Bicocca, Milano, Italy

²¹ Sezione INFN di Milano, Milano, Italy

- ²² *Sezione INFN di Padova, Padova, Italy*
- ²³ *Sezione INFN di Pisa, Pisa, Italy*
- ²⁴ *Sezione INFN di Roma Tor Vergata, Roma, Italy*
- ²⁵ *Sezione INFN di Roma La Sapienza, Roma, Italy*
- ²⁶ *Henryk Niewodniczanski Institute of Nuclear Physics Polish Academy of Sciences, Kraków, Poland*
- ²⁷ *AGH - University of Science and Technology, Faculty of Physics and Applied Computer Science, Kraków, Poland*
- ²⁸ *National Center for Nuclear Research (NCBJ), Warsaw, Poland*
- ²⁹ *Horia Hulubei National Institute of Physics and Nuclear Engineering, Bucharest-Magurele, Romania*
- ³⁰ *Petersburg Nuclear Physics Institute (PNPI), Gatchina, Russia*
- ³¹ *Institute of Theoretical and Experimental Physics (ITEP), Moscow, Russia*
- ³² *Institute of Nuclear Physics, Moscow State University (SINP MSU), Moscow, Russia*
- ³³ *Institute for Nuclear Research of the Russian Academy of Sciences (INR RAN), Moscow, Russia*
- ³⁴ *Budker Institute of Nuclear Physics (SB RAS) and Novosibirsk State University, Novosibirsk, Russia*
- ³⁵ *Institute for High Energy Physics (IHEP), Protvino, Russia*
- ³⁶ *Universitat de Barcelona, Barcelona, Spain*
- ³⁷ *Universidad de Santiago de Compostela, Santiago de Compostela, Spain*
- ³⁸ *European Organization for Nuclear Research (CERN), Geneva, Switzerland*
- ³⁹ *Ecole Polytechnique Fédérale de Lausanne (EPFL), Lausanne, Switzerland*
- ⁴⁰ *Physik-Institut, Universität Zürich, Zürich, Switzerland*
- ⁴¹ *Nikhef National Institute for Subatomic Physics, Amsterdam, The Netherlands*
- ⁴² *Nikhef National Institute for Subatomic Physics and VU University Amsterdam, Amsterdam, The Netherlands*
- ⁴³ *NSC Kharkiv Institute of Physics and Technology (NSC KIPT), Kharkiv, Ukraine*
- ⁴⁴ *Institute for Nuclear Research of the National Academy of Sciences (KINR), Kyiv, Ukraine*
- ⁴⁵ *University of Birmingham, Birmingham, United Kingdom*
- ⁴⁶ *H.H. Wills Physics Laboratory, University of Bristol, Bristol, United Kingdom*
- ⁴⁷ *Cavendish Laboratory, University of Cambridge, Cambridge, United Kingdom*
- ⁴⁸ *Department of Physics, University of Warwick, Coventry, United Kingdom*
- ⁴⁹ *STFC Rutherford Appleton Laboratory, Didcot, United Kingdom*
- ⁵⁰ *School of Physics and Astronomy, University of Edinburgh, Edinburgh, United Kingdom*
- ⁵¹ *School of Physics and Astronomy, University of Glasgow, Glasgow, United Kingdom*
- ⁵² *Oliver Lodge Laboratory, University of Liverpool, Liverpool, United Kingdom*
- ⁵³ *Imperial College London, London, United Kingdom*
- ⁵⁴ *School of Physics and Astronomy, University of Manchester, Manchester, United Kingdom*
- ⁵⁵ *Department of Physics, University of Oxford, Oxford, United Kingdom*
- ⁵⁶ *Massachusetts Institute of Technology, Cambridge, MA, United States*
- ⁵⁷ *University of Cincinnati, Cincinnati, OH, United States*
- ⁵⁸ *University of Maryland, College Park, MD, United States*
- ⁵⁹ *Syracuse University, Syracuse, NY, United States*
- ⁶⁰ *Pontifícia Universidade Católica do Rio de Janeiro (PUC-Rio), Rio de Janeiro, Brazil, associated to ²*
- ⁶¹ *Institute of Particle Physics, Central China Normal University, Wuhan, Hubei, China, associated to ³*
- ⁶² *Institut für Physik, Universität Rostock, Rostock, Germany, associated to ¹¹*
- ⁶³ *National Research Centre Kurchatov Institute, Moscow, Russia, associated to ³¹*
- ⁶⁴ *Instituto de Fisica Corpuscular (IFIC), Universitat de Valencia-CSIC, Valencia, Spain, associated to ³⁶*
- ⁶⁵ *KVI - University of Groningen, Groningen, The Netherlands, associated to ⁴¹*
- ⁶⁶ *Celal Bayar University, Manisa, Turkey, associated to ³⁸*

^a *Universidade Federal do Triângulo Mineiro (UFTM), Uberaba-MG, Brazil*

^b *P.N. Lebedev Physical Institute, Russian Academy of Science (LPI RAS), Moscow, Russia*

^c *Università di Bari, Bari, Italy*

^d *Università di Bologna, Bologna, Italy*

- ^e *Università di Cagliari, Cagliari, Italy*
- ^f *Università di Ferrara, Ferrara, Italy*
- ^g *Università di Firenze, Firenze, Italy*
- ^h *Università di Urbino, Urbino, Italy*
- ⁱ *Università di Modena e Reggio Emilia, Modena, Italy*
- ^j *Università di Genova, Genova, Italy*
- ^k *Università di Milano Bicocca, Milano, Italy*
- ^l *Università di Roma Tor Vergata, Roma, Italy*
- ^m *Università di Roma La Sapienza, Roma, Italy*
- ⁿ *Università della Basilicata, Potenza, Italy*
- ^o *AGH - University of Science and Technology, Faculty of Computer Science, Electronics and Telecommunications, Kraków, Poland*
- ^p *LIFAELS, La Salle, Universitat Ramon Llull, Barcelona, Spain*
- ^q *Hanoi University of Science, Hanoi, Viet Nam*
- ^r *Università di Padova, Padova, Italy*
- ^s *Università di Pisa, Pisa, Italy*
- ^t *Scuola Normale Superiore, Pisa, Italy*
- ^u *Università degli Studi di Milano, Milano, Italy*
- ^v *Politecnico di Milano, Milano, Italy*